phys. stat. sol. (a) **195**, No. 2, 468–474 (2003) / **DOI** 10.1002/pssa.200305950

Giant optical rotation in piezoelectric crystals with calcium gallium germanate structure

R. B. Heimann[*,1], **M. Hengst**[**,1], **M. Rossberg**[***,2], and **J. Bohm**[****,2]

[1] Department of Mineralogy, Freiberg University of Mining and Technology, Brennhausgasse 14, 09596 Freiberg, Germany

[2] Institute for Crystal Growth (IKZ), Max-Born-Strasse 2, 12489 Berlin, Germany

Received by M. S. Brandt 26 June 2002, revised 19 September 2002, accepted 8 November 2002
Published online 24 January 2003

PACS 78.20.Ek, 78.40.Ha

Specific optical rotations ρ in $c(Z)$-direction were measured in single crystals of lanthanum gallium silicon oxide (langasite, $La_3GaGa_3(GaSi)O_{14}$, LGS), as well as its niobium (langanite, $La_3(Ga_{1/2}Nb_{1/2})Ga_3Ga_2O_{14}$, LGN) and tantalum (langataite, $La_3(Ga_{1/2}Ta_{1/2})Ga_3Ga_2O_{14}$, LGT) analogues, and strontium niobium gallium silicon oxide ($Sr_3NbGa_3Si_2O_{14}$, SNGS), all belonging to the calcium gallium germanate structure ($Ca_3Ga(GaGe_2)Ge_2O_{14}$, CGG). The crystals were grown from stoichiometric melts by conventional Czochralski technique and the specific optical rotations obtained by a novel technique via measuring the optical transmission at various wavelengths between crossed polarisers. All compounds investigated show unusually large values of ρ, in particular SNGS.

1 Crystal structure

Crystals of the calcium gallium germanate (CGG) structural family [1, 2] with the general formula $A_3BC_3D_2O_{14}$ crystallise in the acentric crystal class 32 identical to that of α-quartz. However, in contrast to quartz belonging to the enantiomorphic space groups of $P3_121$ (left-handed quartz) or $P3_221$ (right-handed quartz), respectively, the space group of CGG is P321. This space group is, when "empty", not enantiomorphic on its own in contrast to quartz [3]. Hence left- and right-handed forms are being realised in the same space group by appropriate asymmetric, enantiomorphic arrangements of atoms. Instead of a framework of SiO_4 tetrahedra as in quartz which form chiral helical chains resulting in a three-fold screw axis parallel to the crystallographic c-axis, CGG has a layered structure built up from sheets of DO_4 and CO_4 tetrahedra connected by BO_6 octahedra as well as by eight-fold coordinated A atoms (Fig. 1).

Since the cation positions may be occupied or substituted by various aliovalent ions, to date a large number of compounds belonging to the steadily growing CGG structural family have been prepared. The occupation of the cation positions by the constituent ions may be statistical, as in CGG, LGS, LGN, and LGT, or an ordered one, as in SNGS. Hence, CGG shares the structural C position statistically between

[*] Corresponding author: e-mail: heimann@mineral.tu-freiberg.de, Tel.: +49/(3731) 39 2666, Fax +49(3731)39 3129
[**] e-mail: hengstm@mineral.tu-freiberg,de, Tel.: +49 (3731) 39-2172, Fax: +49 (3731) 39-3129
[***] e-mail: rossberg@ikz-berlin.de, Tel.: +49(30) 6392-3091, Fax: +49(30) 6392-3003
[****] e-mail: j.bohm@ikz-berlin.de, Tel.: +49(30) 6797290

© 2003 WILEY-VCH Verlag GmbH & Co. KGaA, Weinheim 0031-8965/03/19501-0468 $ 17.50+.50/0

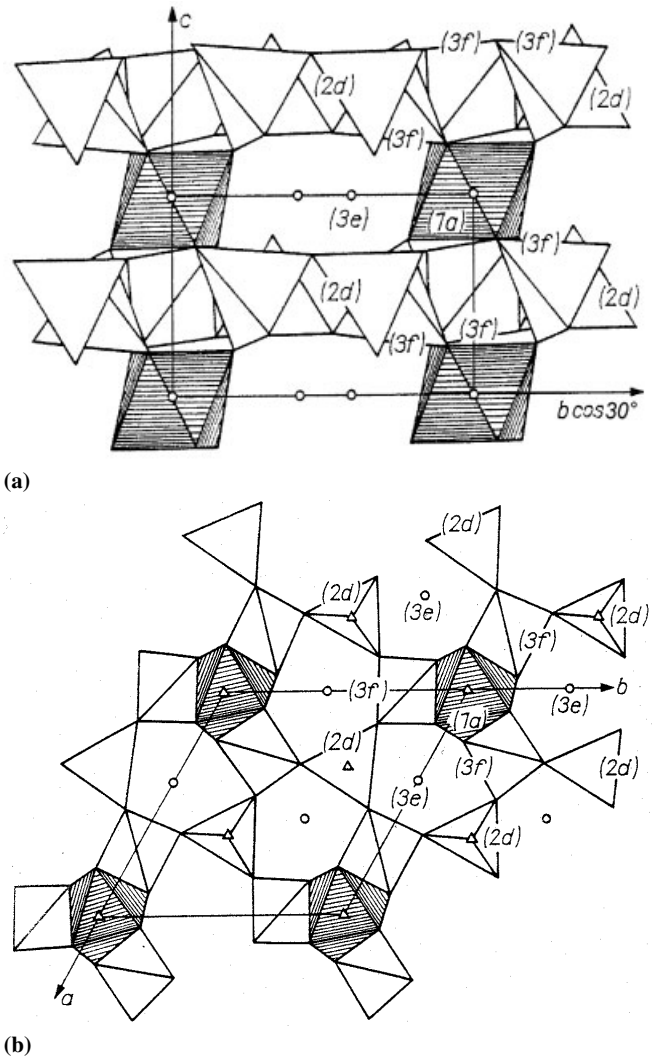

Fig. 1 Projection of the structure of CGG (a) along the $a(X)$-direction, (b) along the $c(Z)$-direction. Positions of cations: A = 3e; B = 1a; C = 3f; D = 2d. Occupation in LGS: La 3e; Ga 1a, 1/2 2d, 3f; Si 1/2 2d (after [2]. Direction of the projected b-axis in (a) corrected in comparison to [2]).

Ga and Ge, LGS the structural D position between Ga and Si, and LGN and LGT share the B position between Ga and Nb, and Ga and Ta, respectively. SNGS shows ordered symmetry with all structurally distinct sites occupied by dissimilar atoms as shown by [4].

2 Growth of single crystals

Single crystals of the CGG structural family were grown by pulling from the melt (Czochralski technique), starting with LGS in the early 1980th [2]. Successfull single crystal growth of SNGS was reported by [5].

In this work, single crystals of LGS, LGN, LGT and SNGS with diameters of about 20 mm and lengths of 60–70 mm were grown by Czochralski technique from their melts using an Oxypuller 05–03 (Cyberstar s.a., Echirolles, France). The iridium crucible used (40 mm ∅ × 40 mm) was equipped with a passive iridium afterheater and heated inductively with a generator of 20 kW at a frequency of 50 kHz. To reduce the oxidation of the iridium the furnace was purged with nitrogen. Process control was achieved through controlling the power output of the generator. The input signal of the control circuit

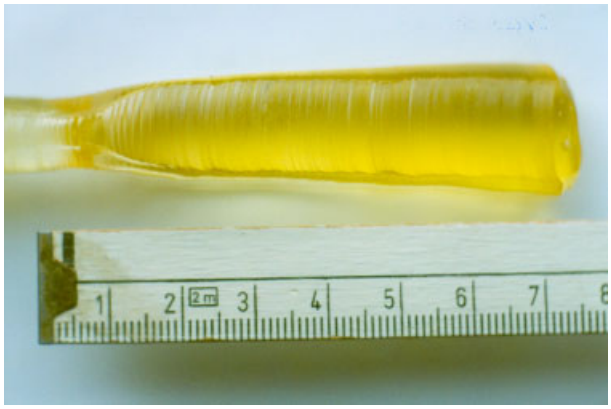

Fig. 2 (online colour at: www.interscience.wiley.com) Single crystal of strontium niobium gallium silicon oxide (SNGS) grown by Czochralski technique along an $a(X)$-axis $\langle 10.0 \rangle$.

was the differential increase of the weight of the growing crystal provided by an electronic balance. The pulling rate was varied between 1 and 3 mm/h and the rotation rate between 10 and 35 r.p.m.

Interestingly, while LGS, LGN, and LGT can be easily grown along their $c(Z)$-axes and with properly oriented seeds also along the Cartesian X- and Y- axes [6], SNGS stubbornly refuses to grow in any orientation direction other than along the polar two-fold a-axis (the Cartesian X-axis) as shown in Fig. 2. The reason for this is still unknown but may be related to the structural differences mentioned above. It should be pointed out that according to the IEEE Standard [7] in an orthogonal system the X-direction corresponds to the direction of the polar two-fold rotation axis $\langle 10.0 \rangle$ and the Y-direction to $\langle 12.0 \rangle$ which is the direction of the bisectrix of a positive and a negative polar two-fold rotation axis.

3 Intrinsic properties

Because of piezoelectric coefficients and electromechanical coupling factors being, respectively, about thrice and twice that of quartz, suitable bulk (BAW) and surface acoustic wave (SAW) phase velocities of LGS, LGN and LGT were measured [6, 8]. Furthermore, since there are no destructive phase transitions between room temperature and their melting points, these compounds are being developed for applications as sensors for pressure, force and acceleration operated at elevated temperatures, SAW band pass filters with low insertion losses, electro-optic devices, and others [9]. The temperature dependences of the dielectric, piezoelectric and electro-optic properties of LGS, LGN and LGT as well as the dispersion of the principal refractive indices of these compounds have been studied by [10]. A pronounced increase of dielectric losses above 350 °C, presumably related to a significant rise of electric conductivity [9] limits the range of operating temperature of these materials. Since phase-matched optical second harmonic generation (SHG) is also possible in these compounds, the search is on to develop compositions with optimised properties in terms of reduced electrical conductivity at high temperature, smaller anisotropy of thermal expansion, and improved temperature-compensated orientations.

In addition, SNGS exhibits an exceptionally large electromechanical coupling factor k of 0.64, about twice as large as that of LGS, LGN or LGT, and five times as large as that of α-quartz, and features also substantially higher intrinsic acoustic Q values [11]. The ordered structure of SNGS may be one reason for this unique behaviour.

4 Measurement of optical activity

The optical activities along the $c(Z)$-axis (optical axis) were measured using a novel technique introduced by [12] and further developed in the course of this work. The optical transmission of an oriented highly polished single crystal bar with thickness d of about 5 mm along the $c(Z)$-direction was measured between crossed polarisers as a function of the wavelength $f(\lambda)$ in the range between 320 and 700 nm for

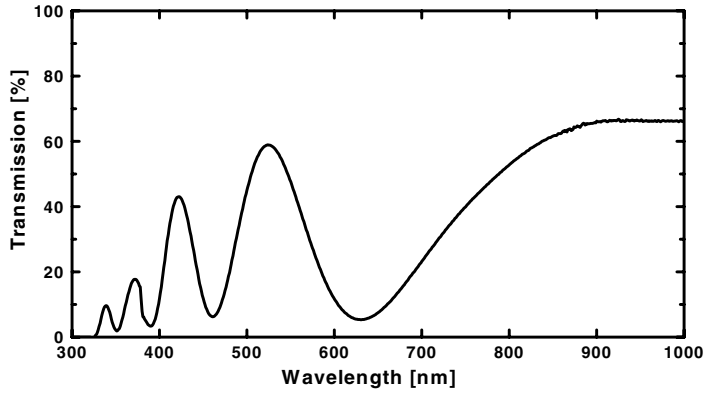

Fig. 3 Optical transmission of SNGS along the *c*(*Z*)-direction as a function of the wavelength ($d = 4.8$ mm).

SNGS, and in the range between 400 and 700 nm for LGS, LGN and LGT, because of their limited transparency. In optically active materials the angle of rotation φ of the vibration plane of linearly polarised light is proportional to the thickness d of the sample or the crystal bar, respectively:

$$\varphi = \rho\, d \tag{1}$$

with the wavelength-dependent specific rotation $\rho(\lambda)$. According to [13] the rotation dispersion of ρ is:

$$\rho = \pi(n_l - n_r)/\lambda_{vac} \tag{2}$$

with the refractive indices n_l and n_r of, respectively, a left-handed and a right-handed circularly polarized wave, and the wavelength λ_{vac} in vacuum. The corresponding curve has a hyperbola-like shape with the specific rotation ρ increasing with decreasing wavelength λ. Hence, when measuring the transmission between crossed polarisers at longer wavelengths, ρ and consequently φ as well as the transmission are rather small. With decreasing wavelengths, ρ and hence φ and the transmission increase, reaching a maximum at $\varphi = 90°$, when the vibration plane of the light is parallel to that of the analyser. At still shorter wavelengths, ρ and hence φ will increase further, but the transmission will decrease, reaching a minimum at $\varphi = 180°$, when the vibration plane of the light is normal to that of the analyser, and so on. In general, maxima will appear when

$$\varphi(\lambda) = \rho(\lambda)d = 90° + m\ 180° \quad (m = 1, 2, 3\ldots)\,, \tag{3}$$

and minima will appear when

$$\varphi(\lambda) = \rho(\lambda)d = m\ 180° \quad (m = 1, 2, 3\ldots)\,. \tag{4}$$

The optical transmission of a crystal bar of SNGS with thickness $d = 4.8$ mm ist shown in Fig 3.

Minima were found at wavelengths of 323, 351, 389, 462, and 629 nm and maxima at wavelengths of 339, 372, 422, and 524 nm. Dividing the angles of rotation φ by 4.8 yields the corresponding specific optical rotations ρ as follows:

	min	max	min	max	min	max	min	max	min
λ [nm]	629	524	462	422	389	372	351	339	323
m	1	1	2	2	3	3	4	4	5
φ [°]	180	270	360	450	540	630	720	810	900
ρ [°/mm]	37.5	56.25	75.0	93.75	112.5	131.25	150.0	168.75	187.5

To determine the handedness of the optical activity, the analyser will be rotated by a certain value α and the measurement repeated. Then, maxima and minima will appear at shifted positions. If the optical

activity has right-handed character and the analyser will be rotated clockwise (when looking towards the analyser) by an angle α_r, than

$$\varphi_r(\alpha_r) = \varphi_r(0) + \alpha_r = \rho_r(\alpha_r)d \tag{5}$$

with φ_r and ρ_r relating to a right-handed optically active crystal. Since $\rho_r(\alpha_r) > \rho_r(0)$ the extrema will be shifted to shorter wavelengths. However, if the analyser will be rotated counter-clockwise by an angle α_l, than

$$\varphi_r(\alpha_l) = \varphi_r(0) - \alpha_l = \rho_r(\alpha_l)d\,. \tag{6}$$

Since $\rho_r(\alpha_r) < \rho_r(0)$ the extrema will be shifted to longer wavelengths.

On the other hand, if the optical activity has left-handed character it follows that

$$\varphi_l(\alpha_r) = \varphi_l(0) - \alpha_r = \rho_l(\alpha_r)d \tag{7}$$

as well as

$$\varphi_l(\alpha_l) = \varphi_l(0) + \alpha_l = \rho_l(\alpha_l)d \tag{8}$$

with the respective meanings of the symbols and the opposite consequences. In case of a numerically low optical activity or a short bar (that means either small ρ or d) one can observe only a few extrema. Nevertheless, by rotating the analyser into some other positions one may gain additional measurement points.

The advantage of the method described here is that the observer has to record only the extrema of the transmission-wavelength curve. This is easier and more accurate than the "classical" technique that relies on determining the exact angle of extinction by rotating the analyser, in particular when the extinction is not complete as occuring in longer samples.

As a control, the specific optical rotations ρ were also measured by the classical technique using interference filters beyond wavelengths of 480 nm on polished disks cut perpendicular to the $c(Z)$-direction.

5 Results

The specific rotations of LGS, LGN, LGT and SNGS determined as described above are displayed in Fig. 4. All crystals investigated rotate clockwise, and hence are right-handed in accordance with the IEEE notation [7].

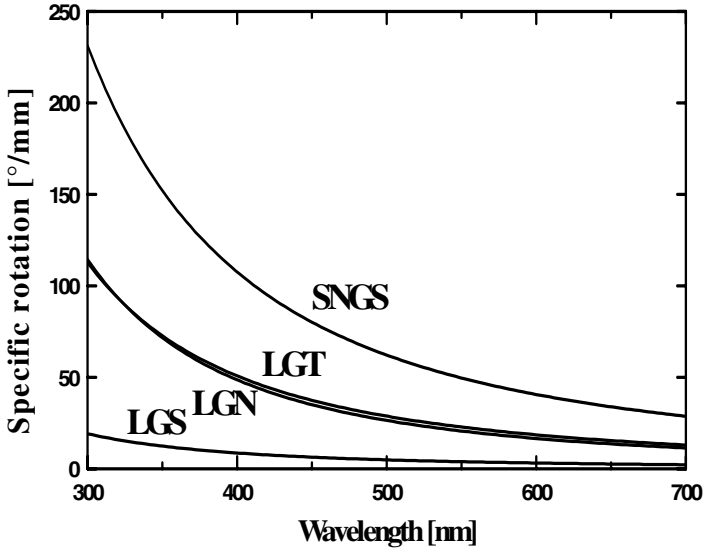

Fig. 4 Specific rotation of LGS, LGT, LGN, and SNGS parallel to the crystallographic $c(Z)$-axis (fits of several measurements to Boltzmann's equation).

The curves for LGN and LGT are nearly identical. The specific rotation ρ of SNGS was found to be unusually large, even when compared to the already rather large specific rotations measured for LGN and LGT. The specific rotation dispersion $\rho(\lambda)$ can be fitted to Boltzmann's equation [14]

$$\rho = A_1/\lambda^2 + A_2/\lambda^4 \,. \tag{9}$$

While the fit uses only two parameters, it is already a rather good one. It resulted in the following coefficients:

	LGS	LGN	LGT	SNGS
A_1 [° nm]	0.9491 (1.0354 [2])	4.526	5.543 (5.558 [12])	12.570
A_2 [° nm^3] $\times 10^{-6}$	0.06996 (0.07695 [2])	0.5207	0. 4136 (0.2657 [12])	0.7428

If λ is given in [nm] the specific rotation ρ is obtained from eq. (9) in [°/nm], and the relation holds: 1°/nm = 10^6 °/mm.

These results are in good agreement with earlier measurements of LGS by [2] and LGT by [12], from whose data the values in parenthesis were calculated. The extrapolation of our fit for LGN to 300 nm yields a specific rotation ρ of 114.6 °/mm that should be compared with a singular ρ value for LGN of 154.5 °/mm at 300 nm given in [15].

5 Summary

Single crystals of LGS, LGN, LGT, as well as SNGS can be grown from stoichiometric melts by conventional Czochralski technique in optical quality. The specific optical rotations ρ in $c(Z)$-direction of relative long samples were obtained by a novel technique via measuring the optical transmission in dependence of the wavelength between crossed polarisers. All compounds investigated show unusually large values of ρ, in particular SNGS. The maximum specific rotation ρ of SNGS was found to be 187.5 °/mm at a wavelength of 323 nm, well above that of quartz. While the value of SNGS is still substantially below that of cinnabar HgS (555 °/mm at λ = 589.3 nm [13]) the transparency, large piezoelectric coefficients, and electro-optic properties of SNGS suggest unique applications including frequency doubling and mixing for electro-optic devices operating at elevated temperatures. Further interesting properties as the Faraday effect and the angular dispersion of phase velocities of surface acoustic waves (SAW) are under investigation.

Acknowledgements The authors are indebted to Drs. J. Donecker and St. Ganschow, Institute for Crystal Growth (IKZ), Berlin, Germany for numerous discussions and valuable experimental advice. A research grant by the Deutsche Forschungsgemeinschaft (DFG) under the contract number He 923/14-1 is gratefully acknowledged.

References

[1] E. L. Belokoneva, M. A. Simonov, A. V. Butashin, B. V. Mill, and N. V. Belov, Dokl. Akad. Nauk SSSR **255**, 1099 (1980).
[2] A. A. Kaminskii, B. V. Mill, G. G. Khodzhabagyan, A. F. Konstantinova, A. I. Okorochkov, and I. M. Silvestrova, phys. stat. sol. (a) **80**, 387 (1983).
[3] J. Bohm and W. Kleber, Wiss. Z. Humboldt-Univ. Berlin, Math.-Nat. Reihe **VIII**, 171 (1958/59).
[4] H. Takeda, J. Sato, T. Kato, K. Kawasaki, H. Morikoshi, K. Shimamura, and T. Fukuda, Mater. Res. Bull. **35**, 245 (2000).
[5] B. V. Mill', E. L. Belokoneva, and T. Fukuda, Zh. Neorganicheskoj Khimii **43,** 1270 (1998) or Russian J. Inorg. Chem. **43**, 1168 (1998).
[6] J. Bohm, E. Chilla, C. Flannery, H.-J. Fröhlich, T. Hauke, R. B. Heimann, M. Hengst, and U. Straube, J. Cryst. Growth **216**, 293 (2000).

[7] IEEE Standard on Piezoelectricity. ANSI/IEEE Standards 176 – 1987, p. 1 – 53, New York (1988).
[8] E. Chilla, C. M. Flannery, H.-J. Fröhlich, and U. Straube, J. Appl. Phys. **90**, 6084 (2001).
[9] J. Bohm, R. B. Heimann, M. Hengst, R. Roewer, and J. Schindler, J. Cryst. Growth **204**, 128 (1999).
[10] J. Stade, L. Bohatý, M. Hengst and R. B. Heimann, Cryst. Res. Technol. **37**, 1113 (2002).
[11] M. M. C. Chou, S. Jen, and B. H. T. Chai, Proc. Ultrasonics Symp., Atlanta, GA, (2001).
[12] J. Donecker, private communication, (1999).
[13] W. Kleber, H.-J. Bautsch, and J. Bohm, Einführung in die Kristallographie, 18. Aufl., S. 297 ff., Berlin: Verlag Technik (1998).
[14] G. Szivessy, Kristalloptik, in: Handbuch der Physik, Eds. H. Geiger and K. Scheel, Berlin (1928).
[15] O. A. Baturina, B. V. Grechushnikov, A. A. Kaminskii, A. F. Konstantinova, B. V. Mill and G. G. Khodzhabagyan, Sov. Phys. – Crystallogr. **32**, 236 (1987).